International Journal of Innovative Computing, Information and Control
Volume **13**, Number **3**, June **2017**

ICIC International ©2017 ISSN 1349-4198
pp. 783–795

REMOTE CONTROL OF OPTICAL SWITCHES FOR WAVELENGTH PATH RELOCATION IN AWG-STAR NETWORKS

Takashi Kojima[1], Osanori Koyama[2], Hiroaki Maruyama[2], Takumi Niihara[2]
Yudai Tomioka[1] and Makoto Yamada[2]

[1]College of Engineering
[2]Graduate School of Engineering
Osaka Prefecture University
Gakuen-cho 1-1, Naka-ku, Sakai, Osaka 599-8531, Japan
{sxb01076; sxb01129; sv106044; swb01119}@edu.osakafu-u.ac.jp
{koyama; myamada}@eis.osakafu-u.ac.jp

Received November 2016; revised March 2017

Abstract. *Given that the number of devices with Internet access continues to rapidly increase, we see Internet traffic also steadily increasing. To accommodate such increases in Internet traffic, various technologies for realizing an expansion of communication capacity and efficiently consuming this capacity are actively being studied. One such technology for expanding communication capacity is wavelength-division multiplexing (WDM), which is applicable not only to large-scale networks but also to local area networks (LANs). An optical device that uses WDM is the arrayed waveguide grating (AWG), which can provide wavelength paths to networks with full mesh topologies. In previous work, we proposed a network that could flexibly relocate wavelength paths employing optical switches for AWGs; however, the network management load was prohibitive because network administrators had to physically go where the optical switches were deployed to control the relocating wavelength paths. In this paper, we propose a remote control system for optical switches to reduce network management load. We evaluated the system performance of our remote control system using experimental networks in which we measured several network parameters. Another goal of our research was to support applications for the Internet of Things (IoT); we used a Raspberry Pi to evaluate our system, as such devices are major candidate IoT devices.*

Keywords: Remote control, Arrayed waveguide grating, Ethernet, IP, Internet of Things, Raspberry Pi

1. **Introduction.** Internet access devices, for example, smartphones, portable PCs, wearable devices, and Internet of Things (IoT) devices are rapidly increasing in prevalence due to substantial progress made in mobile communication technologies and the existing popularization of PCs. Moreover, the amount of digital content available via the Internet is also increasing because of high-definition digital video streaming, voice communication, and so on. Therefore, Internet traffic continues to rapidly increase. According to statistics provided by the Ministry of Internal Affairs and Communications in Japan regarding network traffic, in May 2016, among broadband subscribers, gross download traffic was 6.9 Tbps, which is 1.5 times larger than that of May 2015 and 15 times larger than that of May 2006. Similarly, gross upload traffic was 1.3 Tbps, which is 1.2 times larger than that of May 2015 and 3.3 times larger than that of May 2006 [1].

With these rapid increases in traffic, primary elements in communication networks are changing from metal cables and electrical routers to optical fiber, optical transceivers, wavelength routing devices, and electrical routers. Since optical fiber can transmit a much wider range of frequencies for long distances with low levels of loss versus metal

cables, it is necessary to use optical fiber to realize a new generation of networks in which huge volumes of digital data can be sufficiently transmitted. Moreover, optical networks can expand communication capacity by introducing multiplexing technology using wavelength-division multiplexing (WDM). WDM falls into two categories: Dense WDM (DWDM) and Coarse WDM (CWDM). DWDM is a technology that can multiplex many wavelengths into an optical fiber with very narrow wavelength spacing. And it is used mainly in intercontinental optical fiber networks and domestic core networks. Communication capacity of an optical fiber can be expanded by DWDM extremely but hugely expensive equipment is required. On the other hand, CWDM can multiplex up to 16 wavelengths into an optical fiber. CWDM can be realized employing relatively inexpensive equipment and is used in Metropolitan Area Network (MAN) typically. Various WDM networks have been proposed recently. For example, a network in which CWDM and DWDM can be combined flexibly can hold down initial construction cost by adjusting the mixture fraction of them depending on traffic demands [2]. The introduction of WDM technologies into communication networks has become popular not only in such large-scale networks and MANs, but also in local area networks (LANs), including datacenter networks, campus networks, and networks housed in businesses and buildings. Ethernet remains the most popular standard for LANs; thus optical communication technologies have also been incorporated into Ethernet, achieving transmission speeds of 100 Gbps [3].

Given the above, we proposed allocation methods for communication capacity that depend on traffic demands in Internet Protocol (IP) over Ethernet employing some Optical Add/Drop Multiplexers (OADMs) for CWDM and optical fibers [4-6]. And then, some systems for appropriately allocating communication capacity in the network (for example, IP-routing information supervisory system [7], web-based wavelength path topology design system [8] and IP-routing information control system [9]) were reported. We also demonstrated the validity of our proposals by evaluating several performance measures on experimental networks [4-7,9]. Further, we studied design and control methods for IP over Ethernet using arrayed waveguide gratings (AWGs), which are optical devices that can realize optical fiber networks with huge communication capacity and high-speed transmission.

AWGs can provide many wavelength paths to networks via a full mesh topology. Traffic exchanged between communication nodes is transmitted through these wavelength paths. In previous studies, AWG-based networks have been proposed for wide area networks (WANs) [10,11]; however, these AWG-based networks had problems involving the inefficient consumption of communication capacity due to large fluctuations in traffic demand. This problem occurred because the wavelength path topology of the AWG-based network is fixed. To overcome this problem, a communication capacity allocation method was proposed in [12] that dynamically changes the wavelength path topology by using wavelength-tunable lasers. Unfortunately, this approach was not suitable for use in LANs since wavelength-tunable lasers are expensive and the cost of constructing a LAN should typically be low given that the number of LAN users is also typically relatively low.

Therefore, we proposed an AWG-STAR network that could dynamically relocate wavelength paths by using inexpensive wavelength-fixed optical transceivers, optical switches and OADMs used in [4-9]. The wavelength path relocation was realized by looping back optical signals with control of optical switches manually [13]. We then constructed some experimental networks in our laboratory and demonstrated the performances (throughput, latency, optical loss and so on) on the wavelength path relocation with various traffic patterns on the experimental networks [14]. We also proposed a matrix representation for wavelength path relocation and a calculation method in order to realize a remote network

control system for our AWG-STAR network as a first step [15]. Unfortunately, on our proposed AWG-STAR network, network administrators were required to physically go to where optical switches were deployed to properly control them. Furthermore, there was another problem in terms of traffic management because the administrator could not manage and control the optical switches appropriately on a real-time basis. Thus, a remote control function which can manage and control them in real time is necessary to decrease this network management load.

In this paper, to decrease network management costs in terms of time, the number of workers, and money, we propose a remote control system for wavelength path relocation on optical switches. We also show an implementation using IoT devices. In recent years, application systems employing IoT devices have been the focus of numerous research studies [16-19]; however, to date, few proposed applications are worthy of practical use. We therefore used a Raspberry Pi, a major IoT device, to realize remote control in our AWG-STAR network infrastructure.

In addition to this introductory section, we describe our proposed AWG-STAR network with remotely controlled wavelength paths on IoT devices in Section 2; we also explain wavelength path relocation for controlling optical switches. In Section 3, we show the hardware and software compositions of our remote control system for controlling optical switches with an IoT device. In Section 4, we report system performance on experimental networks that we constructed in our laboratory. Finally, we summarize our conclusions and provide avenues for future work in Section 5.

2. AWG-STAR Network with a Wavelength Path Relocation Function over an IoT Device.

Figure 1 shows an AWG-STAR network with our proposed wavelength path relocation function employing an IoT device. The AWG is an optical device that can output an optical signal to a particular output port according to the optical signal's wavelength. In general, the AWG has n ports for input/output with each port connected to a communication node. For example, a campus building in a university could employ two single-mode optical fibers with one fiber used to transmit optical signals and the other fiber used to receive them.

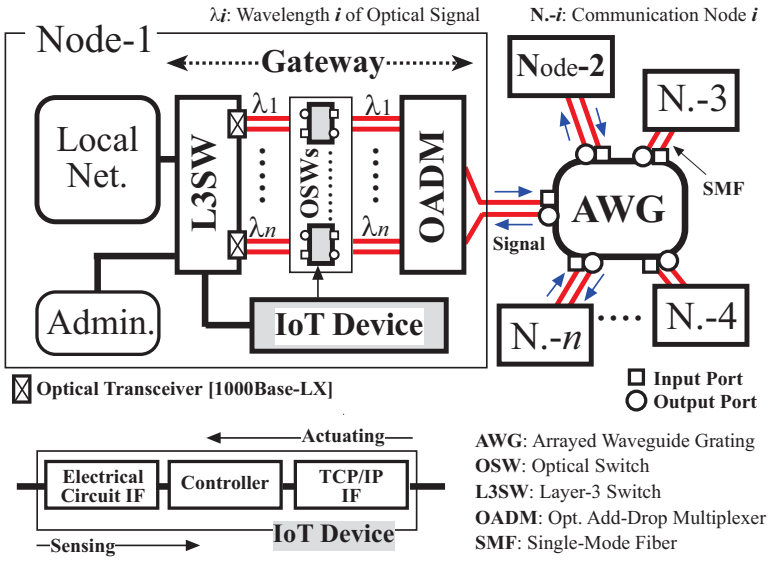

FIGURE 1. AWG-STAR network with a wavelength path relocation function on an IoT device

Each communication node includes several LANs, with each LAN communicating among these LANs with other nodes through a gateway. Here each gateway is composed of a Layer-3 switch (L3SW), n optical switches (OSWs), and an OADM that can route n wavelengths. To control the OSWs, a certain level of electrical voltage must be applied to each OSW. The IoT device shown in Figure 1 can supply the necessary voltage to each OSW. In addition, the IoT device is connected to the L3SW and receives control commands from network administrators through the AWG-STAR network supporting Transmission Control Protocol/Internet Protocol (TCP/IP) and Ethernet.

In general, it is necessary for the IoT device to connect "things" with the Internet. Therefore, the interface on the Internet side requires TCP/IP and Ethernet support. The interface on the "things" side must have a power supply and pulse generation functions to connect itself with electrical circuits. Moreover, the IoT device must have a control function to bridge both sides. In brief, the IoT device requires a "things" actuation function from the Internet and a sensing function that can obtain information from the "things" and output such information to the Internet. In this study, we realized remote control of an optical switch by introducing such an IoT device into the AWG-STAR network.

Figure 2 shows the two states of the terminal connections inside the OSW used in this study; routing for optical signals in each state is also shown. More specifically, the OSW has two internal connection states that establish routes for C_{PT} and C_{LB}. When the state is C_{PT}, connections between the input terminal on the OADM side and the output terminal on the L3SW side and between the output terminal on the OADM side and the input terminal on the L3SW side are available. As a result, optical signals pass through the OSW; as such, the OADM and L3SW can exchange optical signals. Conversely, when the state is C_{LB}, connections between the input and output terminals on the OADM side are available. As a result, optical signals from the input terminal of the OADM side loop back to the OADM.

The state of the OSW can be switched by applying a certain voltage level, which is generated by the IoT device. Figure 2 also shows the OADM functions of multiplexing and splitting optical signals according to the optical signal's wavelength. An OADM supporting n wavelengths can split an optical signal multiplexed over n wavelengths in the input port and can independently output each wavelength to a different port. Conversely,

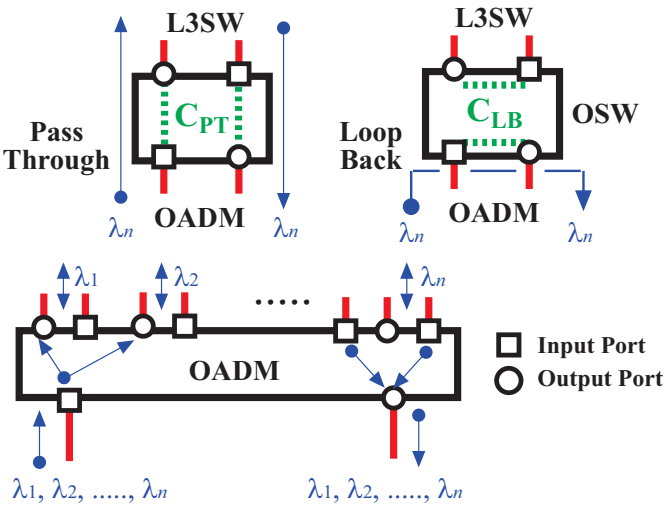

FIGURE 2. Functions of the optical switch (OSW) and optical add/drop multiplexer (OADM)

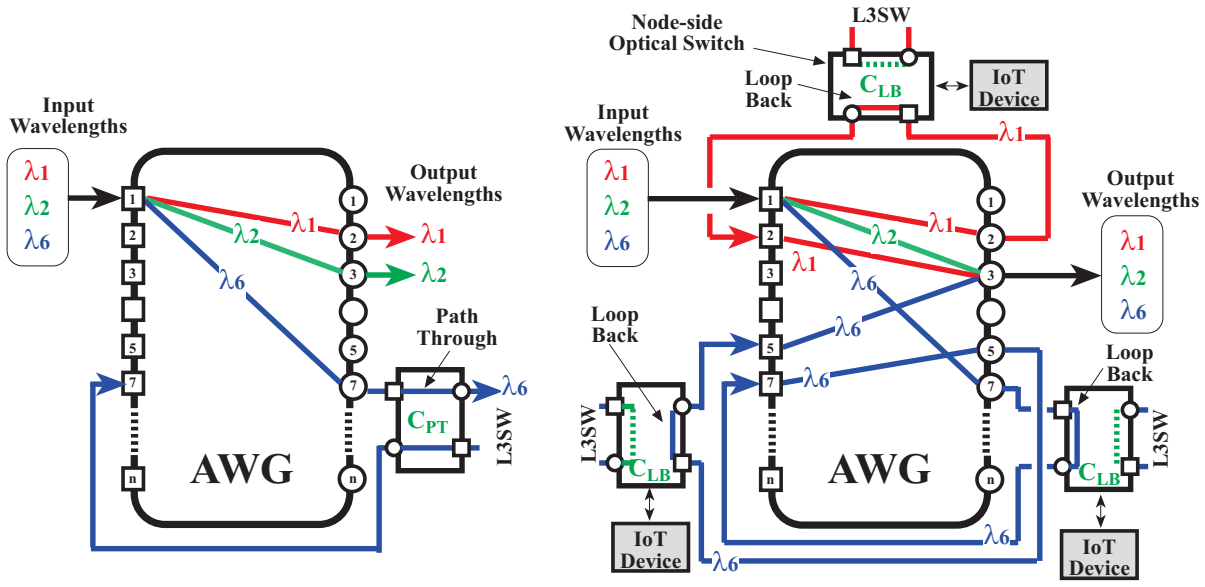

FIGURE 3. Wavelength path relocation by looping back via the OSW

optical signals input from each port corresponding to each wavelength are multiplexed and output as optical signals multiplexed over n wavelengths.

Figure 3 shows the wavelength routing function in the AWG and the increase of communication capacity between nodes via the loopback wavelength. The AWG shown in Figure 3 has a routing function that can support n wavelengths. As shown in the left-hand side of the figure, three wavelengths (i.e., λ_1, λ_2, λ_6) are output to each different port by the wavelength routing function. More specifically, λ_1 is output to port 2, λ_2 is output to port 3, and λ_6 is output to port 7. Each wavelength output from the AWG passes through the OADM (which is omitted from Figure 3) and then reaches the OSW. When the state is C_{PT}, each wavelength passes through the OSW and reaches the L3SW. Conversely, when the state is C_{LB}, a wavelength is looped back at the OSW and is input to the AWG again, as shown in the right-hand side of Figure 3. As an example, λ_1 is output to port 2, and then reaches the OSW via the OADM in node 2. Next, it loops back via the C_{LB} state and goes into the second input port of the AWG. Here, λ_6 is routed similarly and is looped back twice at the OSW.

Each wavelength provides a communication capacity of x bps. For example, λ_2 in the right-hand side of Figure 3 provides a communication capacity of x bps between nodes 1 and 3. Further, λ_1 passes through node 2, and then is output to port 3 because of the wavelength routing function in the AWG. Similarly, λ_6 passes through nodes 7 and 5, and then is output from port 3. The three wavelengths (i.e., λ_1, λ_2, λ_6) input to port 1 are finally output to output port 3, meaning that the wavelength path of λ_1 from node 1 to node 2 and the wavelength path of λ_6 from node 1 to node 7 are relocated between nodes 1 and 3, as shown in the right-hand side of Figure 3. As a result, communication capacity between nodes 1 and 3 is effectively increased by $3x$ bps.

3. **Remote Control System for Wavelength Path Relocation on an Optical Switch.** We focus our study of the remote control system for wavelength path relocation in an optical switch in an AWG-STAR network from two points of view, i.e., as hardware and software compositions. Table 1 shows the OSW specification that we used in our present study. Here, the OSW has four terminals for optical signal transmission, with each set of two terminals used for input and output. There are two states that the

TABLE 1. Specifications of the optical switch (OSW)

Vendor	OMRON Corporation
Model Designation	P1S22B-LD
Terminal	2 (Input) × 2 (Output)
Terminal Connection	C_{PT} and C_{LB}
Drive Voltage for Switching	+5 or −5 [V_{DC}]
Switching Time in Hardware Level	< 4 [ms]
Function	Latching

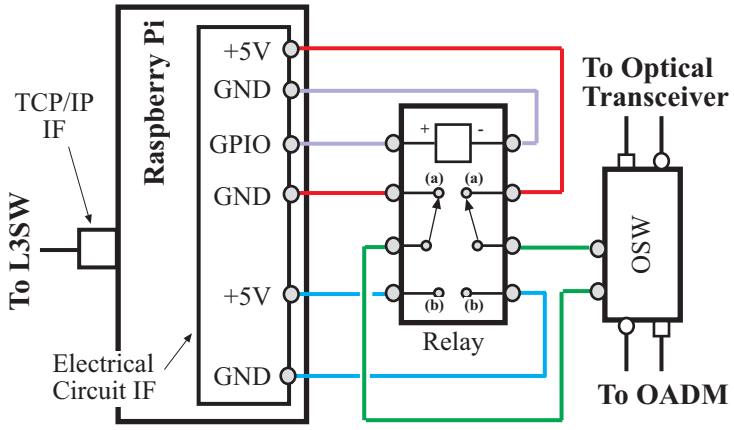

FIGURE 4. Illustrating the connection between the OSW and the Raspberry Pi as IoT device

internal terminals can be in, i.e., C_{PT} and C_{LB}. These two states can be switched by applying 5 V_{DC} to the OSW. Switching time at the hardware level is under 4 ms. In addition, the OSW has a latching function, which can hold state C_{PT} or C_{LB} until an inverse voltage is applied.

To make the OSW controllable through the AWG-STAR network, the OSW needs network communication functionality. Therefore, we connect one or more IoT devices with the OSW. More specifically, we used a single Raspberry Pi as the IoT device for our experiments. Figure 4 illustrates the connection between the OSW and this IoT device. The control command for switching reaches the IoT device through the AWG-STAR network. In accordance with the control command, the IoT device outputs pulses from its general-purpose input/output (GPIO) terminal in the electrical circuit interface (IF), and then switches the connection state in the electrical relay between points (a) and (b) in Figure 4. As a result, the electrical circuit IF supplies +5 V_{DC} to the OSW, causing the connection state in the OSW to switch between C_{PT} and C_{LB}. The relay shown in Figure 4 is a non-latching relay; thus it can switch its connection state only if it receives a pulse from the GPIO terminal. Conversely, the OSW has a latching function and can hold its state until a −5 V_{DC} is applied to the OSW terminals.

To realize the remote control function for the OSW, we designed the system shown in Figure 5. In the figure, network administrators belong to one of the communication nodes and control all of the OSWs in the AWG-STAR network. The administrator inputs control commands through the user IF of the control PC. The command sender then transmits them to the IoT device through the AWG-STAR network via the TCP/IP IF. These commands pass through the AWG-STAR network and reach the TCP/IP IF of the IoT device where the voltage applying selector interprets the commands and the IoT device

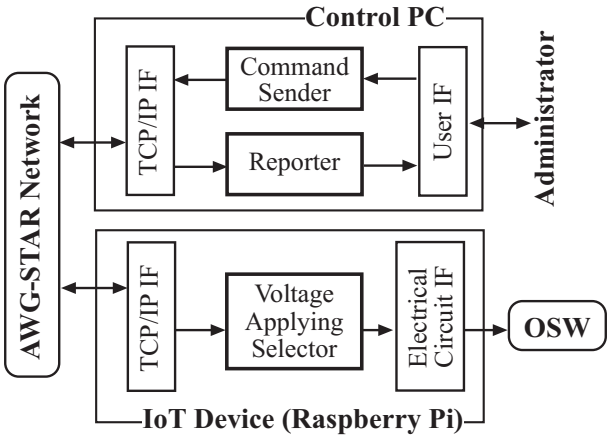

FIGURE 5. Functional module design of our OSW remote control system

TABLE 2. Development environment for our prototype OSW remote control system

	IoT Device	Control PC
Hardware	Raspberry Pi 2 Model B	Mid-level Note-PC
Operating System	Raspbian 4.4.15-v7	Windows 7
Programming Language	Python 3	Python 3

switches the OSW state through the electrical circuit IF based on the control commands received.

Given these hardware and software designs, we implemented our remote control system for wavelength path relocation, using the development environment detailed in Table 2. We also constructed an experimental AWG-STAR network in order to evaluate some performances of the remote control system used in actual network. The remote control system was installed in the experimental network. The performances are shown in detail in Section 4.

4. Performance Experiments on Wavelength Path Relocation with our Remote Optical Switch Control.

4.1. Communication capacity adjustability by wavelength path relocation.

To demonstrate proper optical switching via the remote control function for wavelength path relocation, we measured the change of throughput and packet loss in service traffic. Further, we also measured switching times of the OSW at the network level to estimate the effect OSW switching had on service traffic.

Figure 6 shows the experimental network that we used to measure throughput and packet loss. Further, Table 3 shows the wavelength routing table of the AWG used in our experiments. The AWG had eight input/output ports and could route eight wavelengths (i.e., λ_1: 1610 nm, λ_2: 1470 nm, λ_3: 1490 nm, λ_4: 1510 nm, λ_5: 1530 nm, λ_6: 1550 nm, λ_7: 1570 nm, and λ_8: 1590 nm). In our experiments, we used two of these wavelengths, i.e., λ_2 and λ_3. We installed optical transceivers based on 1000 Base-LX in Ethernet that could send and receive a wavelength in the L3SW. Each optical transceiver used in our experiments could send and receive digital data with transmission speeds of 1 Gbps.

We focused on the throughput and packet loss of service traffic from node 1 to node 3 in our experiments. After wavelength λ_3 was output from node 1, it was routed at the AWG according to wavelength; thus wavelength λ_3 finally reaches node 3. Conversely, wavelength λ_2 reaches node 2 via the AWG after it is output from node 1. Note that node

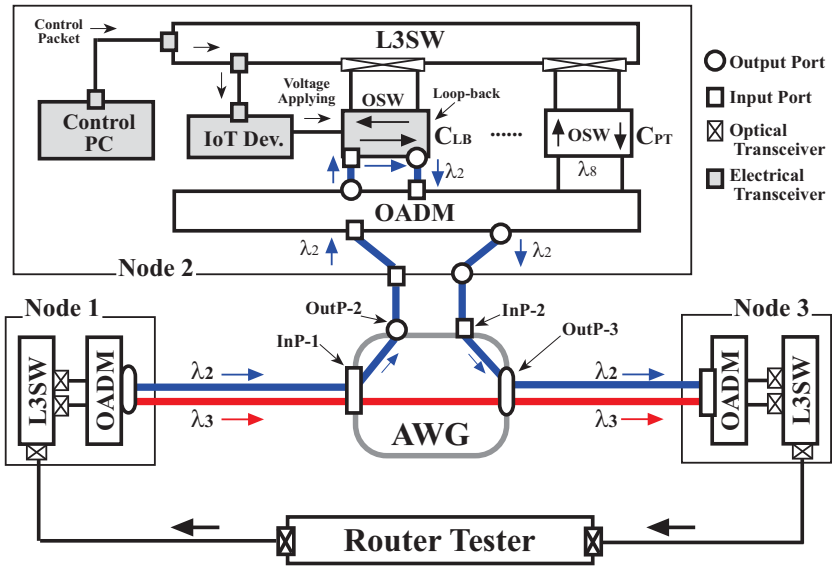

FIGURE 6. Experimental network for the evaluation of throughput and packet loss

TABLE 3. Wavelength routing table for the experimental AWG

AWG Port	OutP-1	OutP-2	OutP-3	OutP-4	OutP-5	OutP-6	OutP-7	OutP-8	Label	Wavelength [nm]
InP-1	λ_1	λ_2	λ_3	λ_4	λ_5	λ_6	λ_7	λ_8	λ_1	1610
InP-2	λ_8	λ_1	λ_2	λ_3	λ_4	λ_5	λ_6	λ_7	λ_2	1470
InP-3	λ_7	λ_8	λ_1	λ_2	λ_3	λ_4	λ_5	λ_6	λ_3	1490
InP-4	λ_6	λ_7	λ_8	λ_1	λ_2	λ_3	λ_4	λ_5	λ_4	1510
InP-5	λ_5	λ_6	λ_7	λ_8	λ_1	λ_2	λ_3	λ_4	λ_5	1530
InP-6	λ_4	λ_5	λ_6	λ_7	λ_8	λ_1	λ_2	λ_3	λ_6	1550
InP-7	λ_3	λ_4	λ_5	λ_6	λ_7	λ_8	λ_1	λ_2	λ_7	1570
InP-8	λ_2	λ_3	λ_4	λ_5	λ_6	λ_7	λ_8	λ_1	λ_8	1590

2 had the remote control system shown in Figure 6. The system could remotely control the OSW deployed as node 2 related to wavelength λ_2. When the state of the OSW was C_{LB}, wavelength λ_2 looped back and was input into the AWG again. After being routed by the AWG, wavelength λ_2 then reached node 3. When the OSW state was C_{PT}, the wavelength path between nodes 1 and 3 was only wavelength λ_3. Conversely, there were two wavelength paths when it was C_{LB}.

We used a router tester shown in Figure 6 as a traffic generator and a network parameter monitor. In this experiment, network parameters included throughput and packet loss in service traffic. Throughput could be estimated by the amount of data received and sent, as measured by the router tester every second. Packet loss could be estimated from the ratio of sent and received IP packets every second. IP packets output from the router tester were equally distributed to each optical transceiver at wavelengths λ_2 and λ_3 at the L3SW in node 1. The wavelengths were multiplexed in the OADM, and then transmitted to the optical fiber between node 1 and the AWG. The wavelengths were also separated at the OADM in node 3, and then input into the optical transceiver at each wavelength in node 3. Finally, IP packets received at the L3SW in node 3 were transmitted and reached the router tester. We switched the OSW corresponding to wavelength λ_2 in node 2 from C_{PT} to C_{LB} while the router tester was transmitting service traffic IP packets

corresponding to a continuous 2 Gbps stream. Finally, the OSW was switched from C_{PT} to C_{LB}, as described next.

The OSW state was switched from C_{PT} to C_{LB} after approximately 60 seconds elapsed from the beginning of our experiments. It was also switched from C_{PT} to C_{LB} at approximately the 120-second mark. The sending-side throughput was approximately 1973 Mbps. It failed to reach 2 Gbps because the traffic router did not count the IP headers as part of these measured data. When the state of the OSW was C_{PT}, there was only wavelength λ_3 traffic between nodes 1 and 3, so the receiving-side throughput was approximately 987 Mbps, as shown in Figure 7. Conversely, when the state of the OSW transitioned to C_{LB}, wavelength λ_2 traffic was added. As a result, the service traffic was distributed into two wavelength paths and the receiving-side throughput increased to approximately 1973 Mbps.

These results show that communication capacity between nodes 1 and 3 expanded due to our wavelength path relocation scheme. This communication capacity expansion can also be understood from the measured IP packet loss, which we show in Figure 8. When there was only wavelength λ_3 traffic between nodes 1 and 3, the loss ratio of IP packets

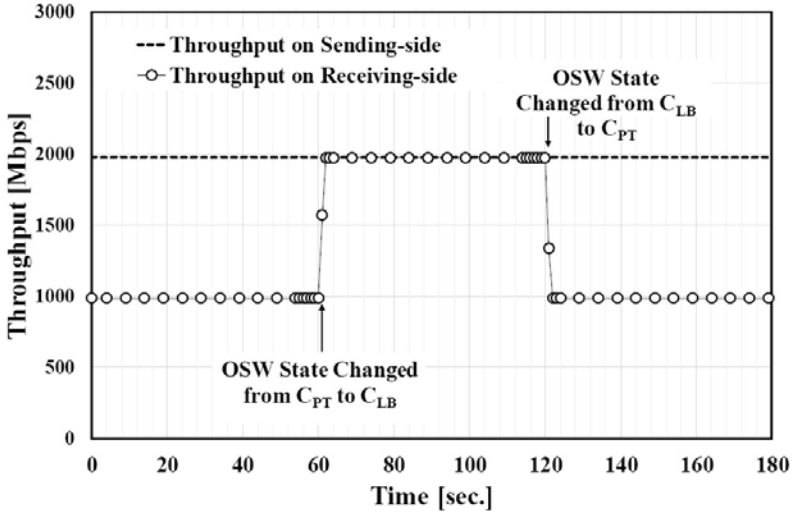

FIGURE 7. Internode communications capacity increase by remote OSW control

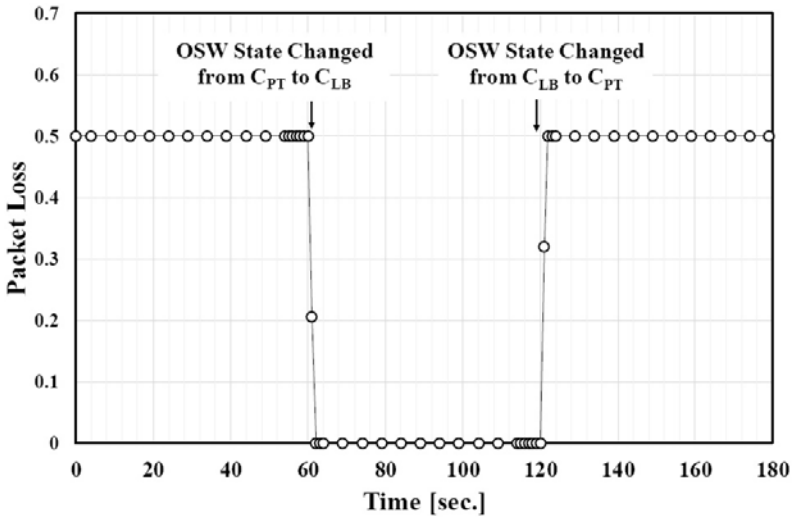

FIGURE 8. Packet loss change by remote OSW control

was approximately 50%. Conversely, when there was traffic for both wavelengths λ_2 and λ_3, no IP packet loss was measured; however, we found that there was a one-second transition between states impacting both throughput and IP packet loss. The cause of the transitions shown in Figures 7 and 8 consisted of a mixture of times in which there were two states, i.e., only wavelength λ_3 and the combined λ_2 and λ_3. These results show that communication capacity can indeed be expanded by remotely controlling the OSW. Also note that the performance of our wavelength path relocation scheme here was equivalent to results obtained without this remote function in our previous research [13,14].

4.2. **Influence of wavelength path relocation on service traffic.** In our experiments, we assumed that there was no service traffic between nodes 1 and 2; however, when it comes to practical use case, service traffic exists in every internode. Therefore, we should evaluate and confirm that our wavelength path relocation scheme influenced service traffic that passed through a relocated wavelength path. This influence could potentially be estimated by measuring switching time of the OSW at the network level; however, we could not measure the switching time because the minimum time resolution of the router tester was one second.

To evaluate the switching time at the network level caused by controlling the OSW remotely, we constructed another experimental network, which we present in Figure 9. In the figure, IP packets that passed through Route A were sent and received by PC-1 and PC-3. Further, transmitted IP packets that passed through Route B were generated by PC-2 and PC-3. By switching OSW-1 and OSW-2 at the same time, either Route A or B could be available. Here, the two OSWs could be controlled by the IoT device. The control PC shown in the figure could control the IoT device by sending control commands.

Further, the L3SW had a mirror port that could copy every packet sent through the L3SW and forward them to a LAN Analyzer. By analyzing the packet capture log saved in the LAN Analyzer, we investigated the behavior of the IP packets on the experimental network. PC-1 and PC-2 continuously sent Echo Request packets based on the Internet Control Message Protocol (ICMP) to PC-3 at 0.03-second intervals. When PC-3 received an Echo Request packet, it replied with an Echo Reply packet. ICMP packets were exchanged between PC-1 and PC-3 when the states of both OSWs shown in Figure 9 were C_1. Conversely, when the states of the OSWs were C_2, ICMP packets were exchanged between PC-2 and PC-3. Under our experimental conditions, we monitored how packet exchanges changed when the states of the OSWs were switched from C_1 to C_2.

Figure 10 shows the measured switching time at the network level due to changes in the OSW state. We confirmed that ICMP packets were exchanged between PC-1 and

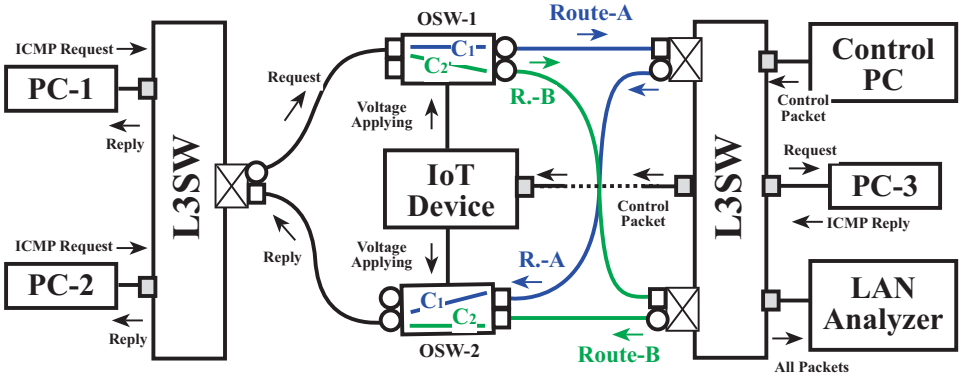

FIGURE 9. Experimental network for evaluating switching time at the network level

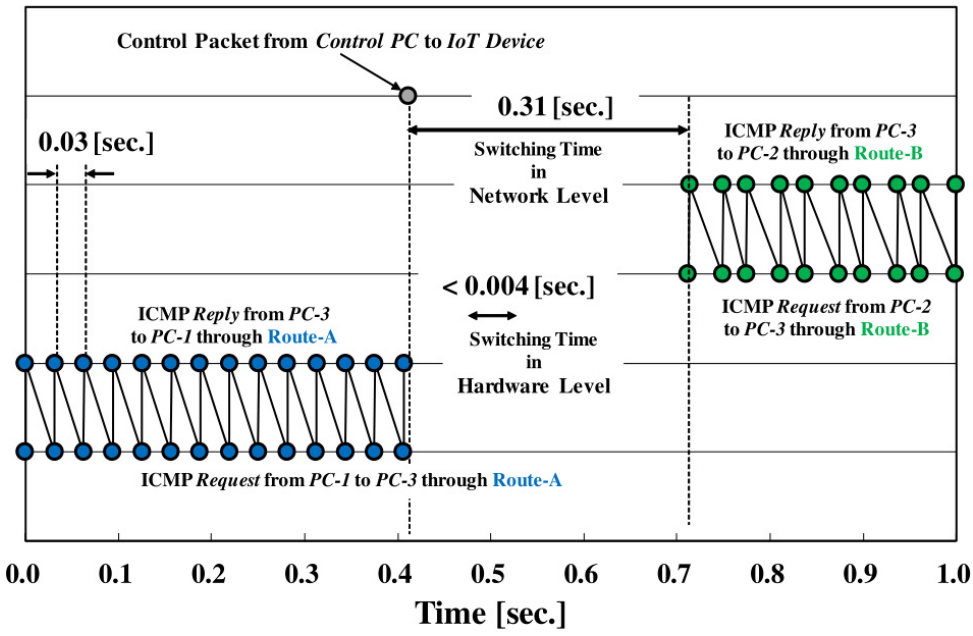

FIGURE 10. Measured switching time in network level

PC-3 while the states of the OSWs were both C_1. At the same time, we also found that there were no ICMP packets exchanged by PC-2 and PC-3 because there was no route between PC-2 and PC-3. After 0.41 seconds from the beginning of our experiment, the control packet was sent by the control PC and the ICMP packet exchange stopped. We found that ICMP packets were exchanged between PC-2 and PC-3 after approximately 0.31 seconds after the control packets were sent.

These results show that Route A was disabled and Route B became available due to the state changes of the OSWs controlled by the IoT device. According to the specifications of the OSW we used, physical internal connections can be switched within 0.004 seconds; however, we clarified that the measured switching time at the network level was as much as 0.31 seconds. Further, we measured the switching time 10 times; as a result, the average switching time was 0.25 seconds.

Consequently, we found that it took approximately 0.25 seconds for wavelength path relocation to occur due to the switching time at the network level. The switching time thus has a potentially negative effect on service traffic due to packet transmission delays during wavelength path relocation. An allowable delay time of a typical service level agreement (SLA) offered by several communication service companies is less than 0.1 seconds, so the delay time caused by wavelength path relocation was slightly above this standard. Therefore, we clarified that service traffic passing through the relocated wavelength path should be diverted onto another wavelength path before wavelength path relocation is conducted.

5. **Conclusions.** In this paper, we proposed a remote control system for OSWs to reduce network management load. The target of our proposed system was the AWG-STAR network that could relocate wavelength paths by changing the OSW state. To realize this remote control for changing the OSW state, we added a network communication function to the OSW by employing a Raspberry Pi as an IoT device. We also implemented software for network administrators that connected with the Raspberry Pi. Further, we constructed an experimental network based on the AWG-STAR to demonstrate the effectiveness of our remote control system. We confirmed that the remote control for the OSW

performed correctly on our experimental network by evaluating the change in throughput and packet loss on service traffic when the state of the OSW was remotely changed. We also constructed another experimental network to evaluate the switching time of the OSW at the network level. We found that the switching time was approximately 0.25 seconds and could cause transmission delays. Therefore, we found it necessary to detour transmitted service traffic via a relocated wavelength path to another wavelength path before we perform wavelength path relocation. We plan to implement such a diverting function for wavelength path relocation without any negative effects on service traffic in our future work. We also showed our remote control system to be an example IoT application since our system included Raspberry Pis.

In future work, the remote control technique proposed in this paper will be applied to traffic monitoring in AWG-STAR network. Furthermore, we will integrate the traffic monitoring function, calculation function for wavelength path relocation with matrix [15] and the remote control function into a Web-based IoT application system.

Acknowledgment. This work was supported by JSPS KAKENHI Grant Number 16K06 306. We thank students in our laboratory for assisting in the construction of the experimental network and for evaluating network performance.

REFERENCES

[1] Ministry of Internal Affairs and Communications, *http://www.soumu.go.jp/main_content/000430359.pdf*, 2016 (in Japanese).

[2] M. Nooruzzaman and E. Halima, Low-cost hybrid ROADM architectures for scalable C/DWDM metro networks, *IEEE Commun. Mag.*, vol.54, no.8, pp.153-161, 2016.

[3] IEEE Computer Society, *IEEE Standard for Ethernet*, Sec.6, p.793, 2012.

[4] M. Nooruzzaman, Y. Harada, O. Koyama and Y. Katsuyama, Proposal of stackable ROADM for wavelength transparent IP-over-CWDM networks, *IEICE Trans. Commun.*, vol.E91-B, no.10, pp.3330-3333, 2008.

[5] O. Koyama, M. Yamada, Y. Okada, K. Matsuyama and Y. Katsuyama, Bidirectional amplification module for IP-over-CWDM ring network, *IEICE Trans. Commun.*, vol.E94-C, no.7, pp.1153-1159, 2011.

[6] M. Nooruzzaman, O. Koyama, M. Yamada and Y. Katsuyama, Scalable single-fiber CWDM ring networks with stackable ROADMs, *IEEE/OSA J. Opt. Commun. Netw.*, vol.5, no.8, pp.910-920, 2013.

[7] S. Fujimoto, T. Sakamoto, K. Nishikawa, T. Onishi, O. Koyama and Y. Katsuyama, Routing information supervisory system in IP-over-WDM ring architecture for customer-owned network application, *International Journal of Innovative Computing, Information and Control*, vol.2, no.2, pp.371-386, 2006.

[8] M. Hashimoto, A. Ueno, M. Taniue, S. Kawase, O. Koyama and Y. Katsuyama, Design and control system over WWW for regional CWDM optical IP networks with reconfigurable optical add/drop multiplexers, *International Journal of Innovative Computing, Information and Control*, vol.4, no.6, pp.1299-1313, 2008.

[9] O. Koyama, K. Toyonaga, M. Yamaguchi, R. Higashiyama and M. Yamada, IP-routing control system for IP/Ethernet over AWG-STAR network, *ICIC Express Letters*, vol.9, no.7, pp.1891-1898, 2015.

[10] K. Noguchi, Scalability of full-mesh WDM AWG-STAR network, *IEICE Trans. Commun.*, vol.E86-B, no.5, pp.1493-1497, 2003.

[11] K. Noguchi, Y. Koike, H. Tanobe, K. Harada and M. Matsuoka, Field trial of full-mesh WDM network (AWG-STAR) in metropolitan/local area, *J. Lightwave Technol.*, vol.22, no.2, pp.329-336, 2004.

[12] O. Moriwaki, K. Noguchi, T. Sakamoto, S. Kamei and H. Takahashi, Wavelength path reconfigurable AWG-STAR employing coprime-channel-cycle arrayed-waveguide gratings, *IEEE Photon. Technol. Lett.*, vol.21, no.14, pp.1005-1007, 2009.

[13] M. Yamaguchi, R. Higashiyama, K. Toyonaga, O. Koyama and M. Yamada, AWG star-network with dynamically reconfigurable wavelength paths via node-side control, *Proc. of OSA Advanced Photonics for Communications*, 2014.

[14] R. Higashiyama, M. Yamaguchi, K. Toyonaga, O. Koyama and M. Yamada, Dynamic enhancement of internode transmission capacity in IP over AWG-STAR network, *Proc. of the 20th APCC*, pp.321-324, 2014.

[15] M. Yamaguchi, O. Koyama, H. Maruyama, T. Niihara and M. Yamada, Matrix representation for wavelength path relocation in AWG-STAR network with loopback function, *International Journal of Innovative Computing, Information and Control*, vol.12, no.3, pp.833-845, 2016.

[16] V. Vujovic and M. Maksimovic, Raspberry Pi as a sensor web node for home automation, *Comput. Electr. Eng.*, vol.44, pp.153-171, 2015.

[17] J. Bermudez-Ortega, E. Besada-Portas, J. A. Lopez-Orozco, J. A. Bonache-Seco and J. M. de la Cruz, Remote web-based control laboratory for mobile devices based on EJsS, Raspberry Pi and Node.js, *IFAC-PapersOnLine*, vol.48, no.29, pp.158-163, 2015.

[18] D. Shaha and V. Bharadib, IoT based biometrics implementation on Raspberry Pi, *Procedia Computer Science*, vol.79, pp.328-336, 2016.

[19] A. J. Lewis, M. Campbell and P. Stavroulakis, Performance evaluation of a cheap, open source, digital environmental monitor based on the Raspberry Pi, *Measurement*, vol.87, pp.228-235, 2016.